POLITECNICO
MILANO 1863

SCUOLA DI INGEGNERIA INDUSTRIALE
E DELL'INFORMAZIONE

Executive Summary of the Thesis

Corrections for k-ω SST to Account for Wall Roughness when Coupled with a Roughness-Induced Transition Model

Laurea Magistrale in Aeronautical Engineering - Ingegneria Aeronautica

Author: Marco Schifone

Advisor: Dr. Barbara Re

Co-advisors: Dr. Andrea Rausa, Francesco Caccia

Academic year: 2024-2025

1. Introduction

In aerodynamics, distributed surface roughness plays a crucial role, as it can trigger an earlier laminar-to-turbulent transition within the boundary layer, with a significant impact on aerodynamic performance. These effects are of great interest in several engineering applications, including wings under icing conditions, gas turbines, and wind turbines. In the latter, power losses, up to 25 %, may be expected due to distributed roughness, typically caused by icing, material erosion [1], or insect impingements [2]. Therefore, the accurate and reliable prediction of roughness-induced transition is a critical aspect of blade design.

In the context of Computational Fluid Dynamics (CFD), Large Eddy Simulation (LES) and Direct Numerical Simulation (DNS) can model roughness-induced transition with high fidelity, as they allow the direct resolution of the roughness elements. However, these methods require an extremely high grid resolution and significant computational resources, making them unsuitable for studying complex 2D and 3D flows. Therefore, the use of correlation-based transition models within the RANS framework is the standard choice for designing and assessing the performance of wind turbine blades. Recent studies have developed an extension of the γ-$\overline{Re_{\theta_t}}$ model to account for surface roughness with the introduction of an additional transport equation for a new variable, called "Roughness Amplification" A_r [3, 4]. In addition, surface roughness can alter the behaviour of the flow near the wall by enhancing momentum exchange, increasing turbulence production, and modifying the effective wall shear stress. To account for all these effects, proper wall boundary conditions must be imposed within the turbulence model, which have been shown to have a major influence on the transition. The standard extension for rough walls proposed by Wilcox [5] for k-ω turbulence models has demonstrated poor accuracy when coupled with Menter's Shear Stress Transport (SST) formulation, due to interference with the SST limiter, as shown by Knopp [6], Aupoix [7], and Hellsten [8]. To cope with this issue, Knopp [6] and Aupoix [7] presented different corrections for rough boundary conditions; their common strategy is to impose finite values at the wall for both the turbulent kinetic energy k and the specific rate of dissipation ω.

The present thesis aims to assess the effects of

boundary conditions for the k-ω SST turbulence model in the presence of surface roughness, when the SST formulation is coupled with a roughness transition model. To the best of the author's knowledge, the problem has not been assessed previously in the literature. Inspired by the work of Langel et al. [4], a roughness transition model has been implemented within the flow solver *SU*2 [9] and validated against flat plate and airfoil test cases. Alongside, Knopp [6] and Aupoix [7] corrections have been implemented and tested against a fully turbulent flat plate. The rough wall corrections have been applied to transitional flows over a flat plate with various pressure gradients and a NACA0012 airfoil with leading edge roughness, showing the accuracy improvements and the limitations of the Wilcox treatment for rough walls. Lastly, this methodology is further extended to a realistic case involving the prediction of the stall behaviour of the NREL-S814, a wind turbine airfoil, under high roughness conditions.
In this executive summary, Section 2 presents an overview of the roughness transition model and the integration of Knopp and Aupoix corrections in the k-ω SST turbulence model. In Section 3, the most relevant results of this work are shown, while Section 4 presents the conclusions of the thesis.

2. Methodology

2.1. Roughness Amplification Model

To accurately model the effects of distributed surface roughness on transitional flows, a roughness amplification model has been implemented within the γ-$\overline{Re_{\theta_t}}$ transition model into the flow solver *SU*2 [9]. The model has been introduced by Dassler et al. [3], and further developed by Langel et al. [4], and it is based on the addition of a transport equation for the roughness amplification A_r, and it is shown in Equation (1):

$$\frac{\partial(\rho A_r)}{\partial t} + \frac{\partial(\rho u_j A_r)}{\partial x_j} = \frac{\partial}{\partial x_j}\left[\sigma_{ar}\left(\mu + \mu_t\right)\frac{\partial A_r}{\partial x_j}\right] \tag{1}$$

The A_r transport equation does not include any explicit source or destruction terms: A_r is produced at the wall, convected through the flow field, and the boundary condition for the roughness variable is shown in Equation (2).

$$A_r\big|_{\text{wall}} = c_{A_r 1} k_s^+, \quad c_{A_r 1} = 8.0 \tag{2}$$

Furthermore, it is necessary to ensure the connection between the roughness amplification variable and the γ-$\overline{Re_{\theta_t}}$ model, which is obtained by modifying the production term in the transition momentum thickness Reynolds number, and consequently decreasing the transported variable $\overline{Re_{\theta_t}}$. The modified production term is presented in Equation (3):

$$P_{\theta_t,\text{mod}} = c_{\theta_t}\frac{\rho}{t}\left[\left(Re_{\theta_t} - \overline{Re_{\theta_t}}\right)\left(1 - F_{\theta_t}\right) - bF_{A_r}\right] \tag{3}$$

where F_{A_r} is a lowering factor that depends on A_r; the polynomial function is composed as a cubic law for low values of the roughness amplification, and a linear growth for higher values. F_{A_r} allows for the decrease of the production term; as a consequence, the transported variable $\overline{Re_{\theta_t}}$ is reduced, and transition is promoted. Moreover, the function b has been introduced to prevent non-physical oscillations for low values of $\overline{Re_{\theta_t}}$. A complete description of all the contents of the model, along with the auxiliary relationships, is detailed in the thesis. In addition, the roughness model has been validated against a 2D flat plate with distributed roughness and with different pressure gradients, along with a NACA0012 airfoil with leading edge roughness. The model has shown good accuracy in both configurations, even if some discrepancies with the reference data are highlighted, because of the lack of a detailed description of the numerical reference studies, and due to the issues related to the standard Wilcox extension for rough walls, as it will be described in Section 2.2.

2.2. k-ω SST Rough Boundary Conditions and Eddy Viscosity Limiters

To account for the effects of surface roughness on the fully developed turbulent boundary layer, additional modifications are needed for the wall boundary conditions of the turbulent variables. Wilcox [5] proposed a modification to the boundary condition of the specific dissipation rate at the wall: the smooth and rough wall boundary conditions are presented in Equa-

tions (4) and (5):

$$\omega_{\text{smooth}} = 10\frac{6\nu}{\beta\,(\Delta y)^2}\,, \quad \text{with:} \quad \beta = 0.09 \quad \text{at} \quad y = 0 \tag{4}$$

$$\omega_{\text{rough}} = \frac{u_\tau^2 S_R}{\nu}\,, \quad \text{with} \quad u_\tau = \sqrt{\frac{\tau_w}{\rho_w}} \quad \text{at} \quad y = 0 \tag{5}$$

where Δy is the height of the first computational cell, S_R is a parameter that depends on the non-dimensional roughness height k_s^+.
According to Knopp [6], Aupoix [7], and Hellsten [8], the Wilcox extension is not suitable when coupled with Menter's SST formulation, and the velocity shift of the logarithmic region, that is, the difference between the solution over a smooth wall and the one for a given roughness correction, is highly underestimated. Figure 1 presents the velocity shift Δu^+ as a function of the non-dimensional roughness height, when Wilcox extension is coupled with the SST formulation, and the Nikuradse correlation is shown as a reference: the shift of the velocity profile shows a significant underestimation for $k_s^+ > 30$.

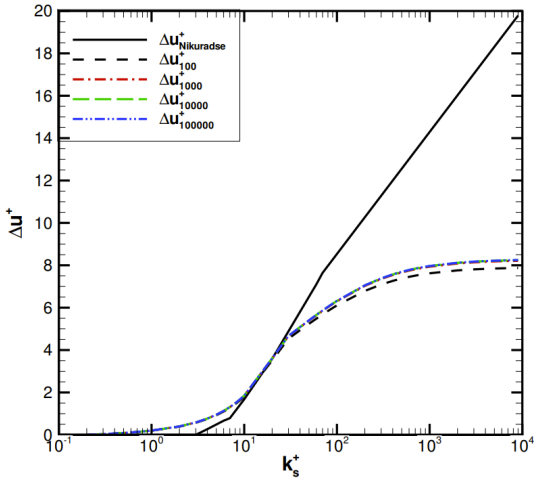

Figure 1: Velocity shift of the logarithmic region as a function of k_s^+, when the Wilcox extension is coupled with k-ω SST [7].

Knopp [6] presented a correction for rough walls by considering finite wall values for both the turbulent kinetic energy k_{wall} and the specific dissipation rate ω_{wall}, based on the assumption that the eddy viscosity in the log layer can be modelled as shown in Equation (6):

$$\nu_{\text{t,log}} = u_\tau \kappa\,(y + d_0) \tag{6}$$

The boundary conditions at the wall for the Knopp extension are presented in Equation (7):

$$k_{\text{wall}} = \frac{u_\tau^2}{\sqrt{\beta^*}}\min\left(1, \frac{k_s^+}{90}\right)$$
$$\omega_{\text{wall}} = \min\left(\frac{u_\tau}{\sqrt{\beta^*}\kappa\tilde{d_0}}, 10\frac{6\nu}{\beta\,(\Delta y_1)^2}\right) \tag{7}$$

The Knopp extension provides relevant improvements compared to the standard Wilcox wall treatment; however, the velocity shift results in a slight underestimation throughout the fully rough regime.
To cope with the issues related to the Wilcox extension and the problems of the Knopp correction, Aupoix [7] presented a new correction: the basic idea to obtain the correct velocity shift is to impose the solution over a smooth wall at a certain distance from the wall y_0, where the velocity is equal to the required velocity shift $\Delta u^+(y_0^+)$. This correction allows for matching the velocity shift of the corresponding correlation exceptionally well, as shown in Figure 2, while the complete boundary conditions are presented in the thesis.

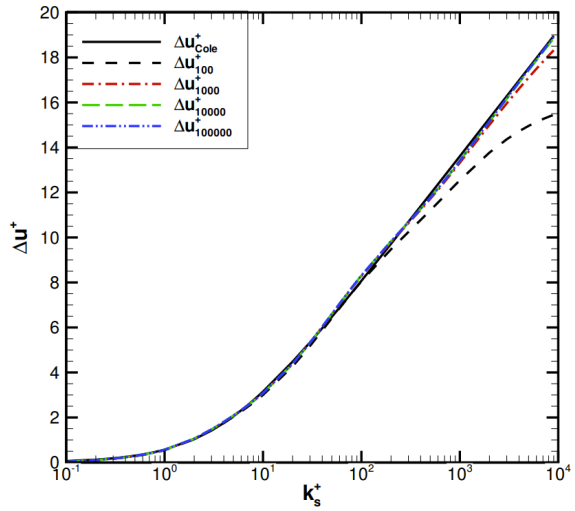

Figure 2: Velocity shift of the logarithmic region as a function of k_s^+, when the Aupoix extension is coupled with k-ω SST [7].

The Knopp and Aupoix corrections have been implemented into *SU2*, and their effects have been verified against a fully turbulent flat plate.

3. Results

The roughness transition model, coupled with different boundary conditions for k-ω SST, is tested with different test cases: a flat plate with distributed roughness, a NACA0012 airfoil with leading edge roughness, and an NREL-S814 airfoil under high roughness conditions, allowing a direct comparison between the Wilcox wall treatment and the eddy viscosity corrections.

3.1. Flat Plate with Distributed Roughness

The first test case involves a flat plate with distributed roughness under several pressure gradients. In this section, the results of the Zero Pressure Gradient (ZPG) will be presented, and the complete results are detailed in the thesis.
The free stream velocity is set to $20\,m/s$, the free stream turbulence intensity (FSTI) is $1.1\,\%$, with a temperature of $T_\infty = 300\,K$. The flat plate extends for $0.15\,m$ upstream of the leading edge of the plate, and for $1\,m$ downstream. The computational mesh, selected after a grid independence study, features 587 points in the streamwise direction, and 123 in the wall-normal direction. The first cell height is set to $\Delta y/c = 1.25 \times 10^{-7}$, which allows for obtaining an average value of $y^+ \approx 0.005$.
A crucial parameter is the transition onset location, which is defined as the point where the skin friction coefficient C_f reaches the minimum value; this information is used to compute the transition onset Reynolds number ($Re_{x_t} = \rho U_\infty x_t/\mu$), which is plotted in Figure 3 against the roughness Reynolds number ($Re_{k_s} = \rho U_\infty k_s/\mu$).

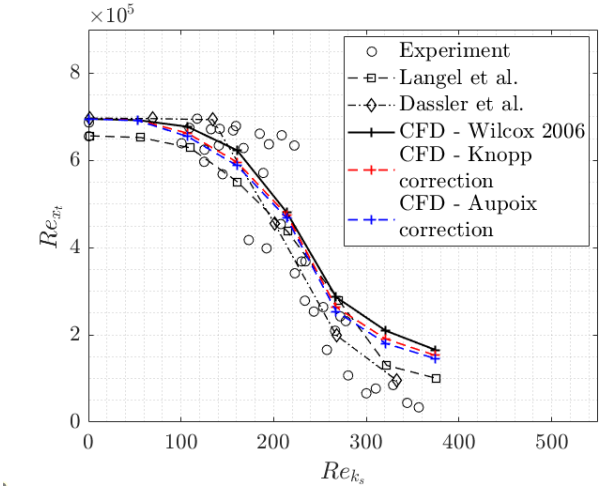

Figure 3: Effect on Re_{x_t} of different wall treatments when coupled with the k-ω SST turbulence model.

As noted in previous studies by Dassler et al. [3] and Langel et al. [4], and confirmed with numerical simulations, the transition is not significantly affected by surface roughness for $Re_{k_s} < 120$. For this range, the variation in the transition onset location is negligible, as depicted in Figure 3. When the Wilcox extension is employed, the general behaviour of Re_{x_t} is in good agreement with both the experimental data and the numerical results as long as $Re_{k_s} < 260$. A consistent discrepancy is highlighted for higher values of the roughness Reynolds number, where the transition onset location is not sufficiently displaced upstream.
In the present test case, when the eddy viscosity corrections are applied, the earlier onset of the transition that is triggered ensures a slight improvement of the solution, even if in the last part of the range being tested, that is for $k_s > 260$, the behaviour of Re_{x_t} still presents a slight overshoot. However, it has also to be mentioned that the whole range of roughness levels tested in this configuration lies within the transitionally rough regime ($5 < k_s^+ < 70$). At the same time, it has been shown in Section 2 that the most significant discrepancies between the Wilcox extension and the eddy viscosity limiters lie in the fully rough regime.

3.2. NACA0012 with LE Roughness

A further test case, to show the effects of different boundary conditions on k-ω SST coupled with the roughness transition model, involves

a NACA0012 airfoil with LE roughness. The experimental results of Kerho and Bragg [10] are used to assess the behaviour of the boundary conditions for rough walls. Several extents of surface roughness are applied to three different chordwise locations, and the velocity profiles within the boundary layer have been measured at various locations on the airfoil surface.

The chord of the profile is $c = 0.5334\,m$, the free stream Reynolds number, based on the chord of the profile, is set to $Re_\infty = 1.25 \times 10^6$, with an $FSTI = 0.1\,\%$, Mach number of 0.1, and free stream temperature of $T_\infty = 288.15\,K$.

The computational mesh features an O-grid topology, and, after a grid independence study, 883 points were used on the airfoil surface, with a finer distribution near the leading and trailing edges. The first cell height is $\Delta y/c = 1.25 \times 10^{-6}$, with a growth rate of 1.125, which returns 132 elements in the wall-normal direction.

To verify the effects of surface roughness on the boundary layer development process, the velocity profiles obtained with the Wilcox [5], Knopp [6] and Aupoix [7] extensions are compared to the experimental results of Kerho and Bragg [10]. They are shown in Figures 4, 5 and 6. When the Wilcox extension is used, the roughness model agrees well with the experimental results; however, a discrepancy can be highlighted in the first locations for all three roughness configurations, where the velocity profiles exhibit typical laminar boundary layer behaviour, indicating that the predicted boundary layer development is delayed compared to the experiments.

These issues can be addressed by applying the eddy viscosity corrections. In the first two roughness cases (Figures 4 and 5), the Knopp extension for k-ω SST introduces slight improvements, in particular in the first two stations presented for each roughness configuration. In contrast, Aupoix correction allows for the velocity profiles of the experimental results to be matched exceptionally well throughout all the stations shown. In the last configuration (Figure 6), roughness has been applied further downstream from the leading edge. The most significant improvement, in this case, is highlighted between $x/c = 0.15$ and $x/c = 0.2$, where both Knopp and Aupoix corrections effectively reproduce the physical behaviour of the boundary layer. In contrast, at $x/c = 0.1$, the discrepancy between experimental and numerical results remains unchanged.

Also in this test case, even if the non-dimensional roughness height is not particularly high, being $k_s^+ \approx 30$, hence in the transitionally rough regime, the use of eddy viscosity limiters has been shown to improve the numerical accuracy of the roughness model. This test case assessed the robustness and reliability of the roughness corrections on airfoil configurations.

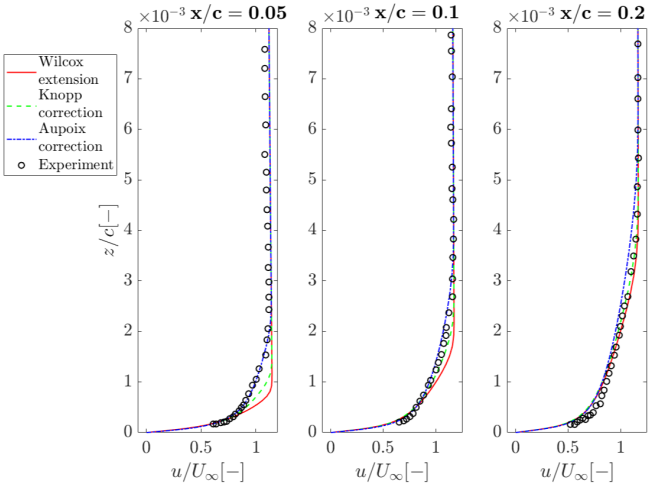

Figure 4: Boundary layer profiles with surface roughness applied at $x/c = 0.00187 - 0.0191$, comparison with Kerho and Bragg experimental results [10].

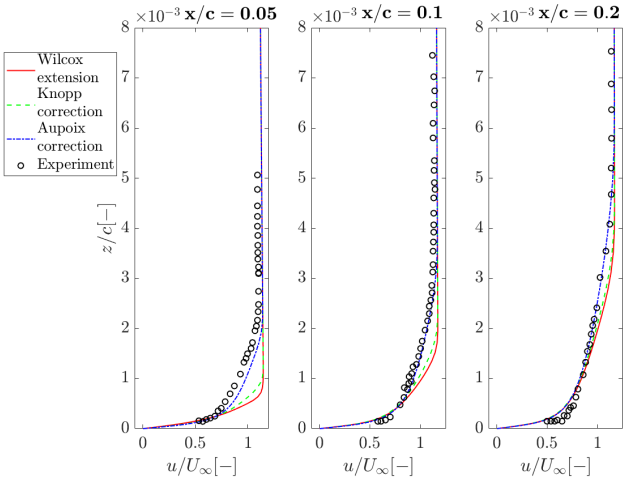

Figure 5: Boundary layer profiles with surface roughness applied at $x/c = 0.00612 - 0.0258$, comparison with Kerho and Bragg experimental results [10].

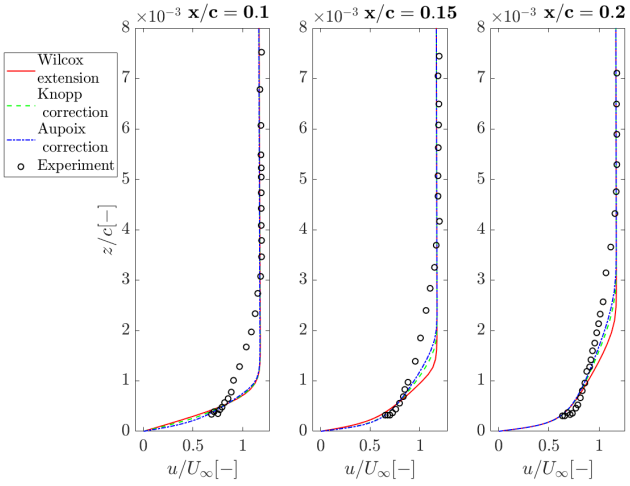

Figure 6: Boundary layer profiles with surface roughness applied at $x/c = 0.0314 - 0.0539$, comparison with Kerho and Bragg experimental results [10].

3.3. Stall Behaviour of the NREL-S814 with Large LE Roughness

To provide a more accurate description of the effects of the eddy viscosity corrections on transitional flows coupled with k-ω SST, the NREL-S814 airfoil, developed for wind turbine applications, has been investigated under high roughness conditions. The NREL-S814 airfoil with surface roughness has been tested by Janiszewska et al. [11] at a free stream Reynolds number of $Re_\infty = 1.5 \times 10^6$, based on the chord length, Mach number of 0.1, and free stream temperature of $T_\infty = 288.15\,K$. The profile chord is $c = 0.457\,m$, while, based on average particle size from the field specimen, standard #40 grit was chosen for the roughness elements, returning $k_s/c = 0.0019$. The rough region extends for $0.223c$ starting from the leading edge and is applied to both the pressure and suction sides. The $FSTI$ was set to 0.2 %, and the S814 airfoil has been tested for angles of attack from $-4°$ to $15°$.

The computational mesh features an O-grid topology, and after a grid independence study, 1827 points have been selected on the airfoil surface, and 178 in the wall-normal direction. The growth rate is set to 1.1, while the first cell height is $\Delta y/c = 2.5 \times 10^{-7}$.

Figures 7 and 8 present the C_l-α and drag polar curve, respectively, and the effects of different boundary conditions are compared to the experimental results by Janiszewska et al. [11]. The Wilcox extension shows good agreement with the experimental data for moderate angles of attack, that is, between $-4°$ and $6°$, but fails in predicting the behaviour of the flow near stall, with a consistent overshoot of the maximum lift coefficient, stall angle, and drag coefficient under these conditions. This behaviour can be explained by considering that the flow is in the fully rough regime, with $k_s^+ \approx 220$, and significant discrepancies are expected when the Wilcox extension is coupled with the SST formulation. When the Knopp and Aupoix corrections are used, the behaviour near stall significantly improves, and it can be accurately predicted with the Aupoix limiter: both the C_l-α and the Cl-C_d curves present a good fit with the experimental results, showing the major improvements obtained with the eddy viscosity limiters in stall conditions. However, discrepancies in the lift coefficient can be detected for $-4° < \alpha < 6°$, with an overestimation of the drag coefficient in this range.

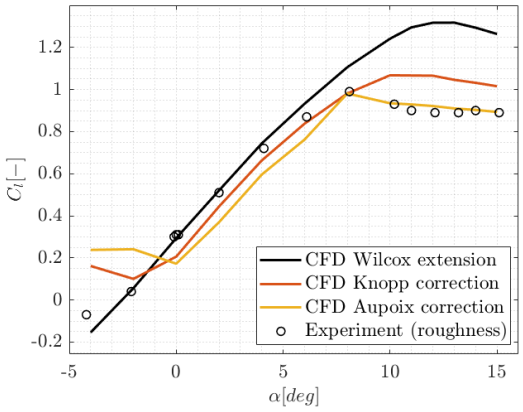

Figure 7: Effects of the Wilcox, Knopp and Aupoix boundary conditions on C_l-α curve of the NREL-S814, compared to the experimental results [11].

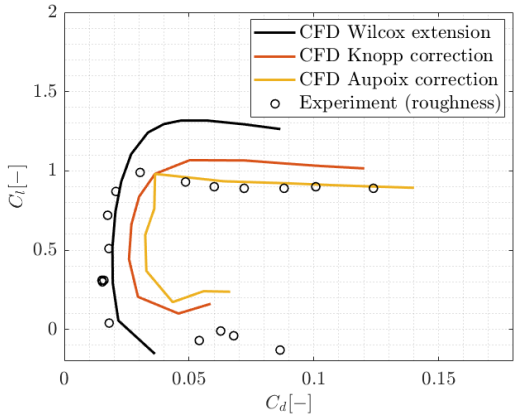

Figure 8: Effects of the Wilcox, Knopp and Aupoix boundary conditions on C_l-C_d curve of the NREL-S814, compared to the experimental results [11].

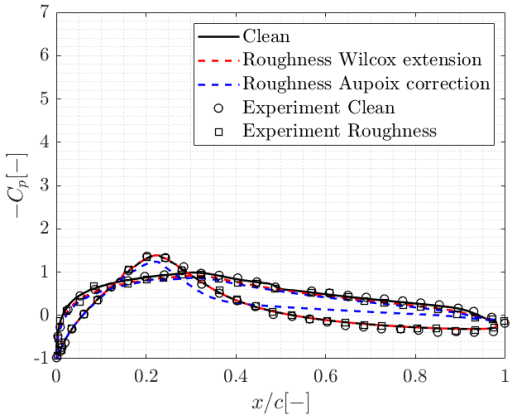

Figure 9: Comparison of the predicted C_p plot at $\alpha = 0°$ with the experimental results [11].

This issue could lie in the aerodynamic properties of the NREL-S814 airfoil, which is designed to be insensitive to surface roughness. Figure 9 shows the C_p plot for $\alpha = 0°$, when the Wilcox and Aupoix extensions are used, and the experimental results are presented as a reference. The experimental plots suggest that the difference between the clean and rough configurations is minimal, and the NREL-S814 appears to be insensitive to surface roughness for moderate angles of attack. Under these conditions, the Wilcox extension presents good agreement with the experiments, while the Aupoix correction presents issues on the pressure side, where the pressure gradient turns into adverse. Regarding this discrepancy, it has to pointed out that the roughness corrections have been calibrated on flat plates test cases, and, even though it has been previously shown how they can improve accuracy on flat plates and airfoils with moderate pressure gradients, they have not been tested in the presence of rapid variations of the pressure gradient, as it happens on the S814 airfoil at moderate angles of attack.

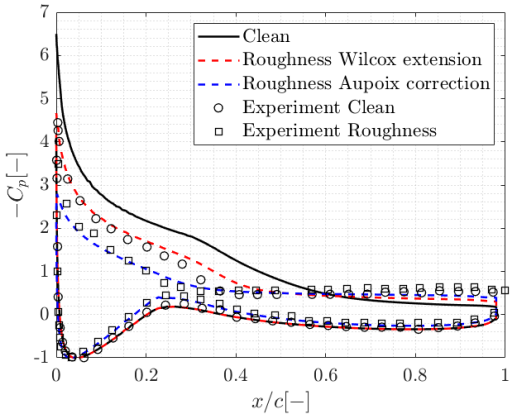

Figure 10: Comparison of the predicted C_p plot at $\alpha = 15°$ with the experimental results [11].

The numerical accuracy of the model increases with angle of attack, where it is also noticed that the steep change in the pressure gradient on the bottom surface of the airfoil starts to be smoothed out. Around stall conditions, the roughness model coupled with the Aupoix correction matches exceptionally well the experimental behaviour of the C_p, as shown in Figure 10, where the predicted pressure coefficient at $\alpha = 15°$ is plotted. In this configuration, the Wilcox extension presents a major discrepancy with the reference data, particularly on the suction side of the airfoil, which explains the inaccuracy in predicting the behaviour of the flow near the stall.

In conclusion, given the limitation of the eddy viscosity limiters and the peculiar aerodynamic characteristics of the airfoil, the stall behaviour can be predicted with enhanced accuracy when

the roughness transition model is coupled with the Knopp and Aupoix corrections.

4. Conclusions

This present work has investigated the effects of rough wall boundary conditions for k-ω SST, when coupled with a transition model. The study began with the implementation of a roughness transition model, following the work of Langel et al. [4], which has been validated against several test cases.
However, when the Wilcox [5] extension is coupled with the SST formulation, significant discrepancies are highlighted in the velocity profiles of the logarithmic region, and the velocity shift is highly underestimated.
Two alternative rough wall treatments were introduced and implemented to address these shortcomings: the Knopp [6] and the Aupoix [7] corrections. When these corrections were coupled with the roughness transition model and applied to transitional flows over flat plates and a NACA0012 airfoil, a significant improvement was observed. Moreover, the Aupoix correction has demonstrated the most consistent performance, especially in fully rough conditions. Lastly, the methodology was extended to a more practical application: the stall behaviour of the NREL-S814 airfoil under high roughness conditions. Results indicated that including eddy viscosity limiters enhanced the accuracy of stall predictions, making these corrections highly relevant for industrial applications involving surface degradation or contamination.

References

[1] A. Sareen, C. A. Sapre, and M. S. Selig. Effects of Leading Edge Erosion on Wind Turbine Blade Performance. *Wind Energy*, 17(10):1531–1542, 2014.

[2] G. P. Corten and H. F. Veldkamp. Aerodynamics: Insects Can Halve Wind-Turbine Power. *Nature*, 412(6842):41 – 42, 2001.

[3] P. Dassler, D. Kozulovic, and A. Fiala. Modelling of Roughness-Induced Transition Using Local Variables. In *European Conference on Computational Fluid Dynamics*, 2010.

[4] C. Langel, R. Chow, C.P. van Dam, D. Maniaci, R. Ehrmann, and E. White. A Computational Approach to Simulating the Effects of Realistic Surface Roughness on Boundary Layer Transition. *52nd AIAA Aerospace Sciences Meeting - AIAA Science and Technology Forum and Exposition, SciTech 2014*, 2014.

[5] D. Wilcox. *Turbulence Modeling for CFD (Third Edition)*. DCW Industries, 2006.

[6] T. Knopp, B. Eisfeld, and J. B. Calvo. A new extension for k–ω turbulence models to account for wall roughness. *International Journal of Heat and Fluid Flow*, 30(1):54–65, 2009.

[7] B. Aupoix. Wall Roughness Modelling with k-ω SST Model. In *10th International ERCOFTAC Symposium on Engineering Turbulence Modelling and Measurements*, 2014.

[8] A. Hellsten and S. Laine. Extension of the k-ω SST Turbulence Model for Flows over Rough Surfaces. *AIAA Journal*, 36:1728–1729, 1998.

[9] F. Palacios, M. Colonno, A. Aranake, A. Campos, S. Copeland, T. Economon, A. Lonkar, T. Lukaczyk, T. Taylor, and J. Alonso. Stanford University Unstructured (SU2): An Open-Source Integrated Computational Environment for Multi-Physics Simulation and Design. *AIAA Journal*, 2013.

[10] M. F. Kerho and M. B. Bragg. Airfoil Boundary-Layer Development and Transition with Large Leading-Edge Roughness. *AIAA Journal*, 35(1), 1997.

[11] J. M. Janiszewska, Reuss Ramsay R., M. J. Hoffmann, and Gregorek G. M. Effects of Grit Roughness and Pitch Oscillations on the S814 Airfoil. *National Renewable Energy Laboratory*, 1996.